Climatology and recent increase of westerly winds over the Amundsen Sea derived from six reanalyses

Thomas J. Bracegirdle

British Antarctic Survey, Cambridge, United Kingdom

Prepared for the International Journal of Climatology

Short title: Winds over the Amundsen Sea

23 January 2012

Full author address:

British Antarctic Survey, Cambridge, UK, CB3 0ET

e-mail: tjbra@bas.ac.uk

tel: +44 (0) 1223 221571

fax: +44 (0) 1223 362616

Abstract

The observed acceleration of glaciers from West Antarctica into the Amundsen Sea is estimated to be contributing 6% to current sea-level rise with the estimated potential to add 0.24 m to global sea level. Stronger westerly winds over the Amundsen Sea can increase the flow of relatively warm ocean water to the base of ice shelves that flow from glaciers into the Amundsen Sea. Thinning of the glaciers caused by this warming is a potentially important factor in driving the observed acceleration of glaciers. However, the climatology of winds in the region has not been extensively studied due to a lack of in-situ observational long-term records. Here six different reanalysis datasets are assessed (CFSR, ERA-40, ERA-Interim, JRA-25, MERRA and NNR1) to determine a best estimate of variability and change since 1979 when the widespread monitoring of the atmosphere from satellites was introduced. A comparison with independent mean sea level pressure (MSLP) data from ice drifting buoys shows that ERA-Interim is clearly the most accurate at capturing the details of individual weather systems over the neighbouring Bellingshausen Sea, implying that it is also accurate over the Amundsen Sea. In terms of climatological means, the five recently-produced (after ~2000) reanalysis datasets show only small differences. Decadal variations of westerly winds congruent with the observed increases in the southern annular mode (SAM) index are a consistent feature across the reanalysis datasets. In particular, the strong seasonal dependence of observed trends in the SAM (i.e. significant positive trends in the summer and autumn in recent decades) is also seen in the strength of westerly winds over the Amundsen Sea. In terms of year-to-year variability, the annual mean westerly winds over the Amundsen Sea were found to be significantly correlated with the SAM in summer ($r=0.35$; $p\leq0.05$) and ENSO in spring (September-November) ($r=0.41$; $p\leq0.05$).

1. Introduction

The Amundsen Sea Embayment (ASE) is a location where glaciers (principally the Pine Island and Thwaites glaciers) are observed to have been thinning in recent decades (Shepherd et al., 2001). This thinning is associated with an acceleration of flow into the ocean (Rignot et al., 2008). The additional ice entering the ocean is estimated to be contributing approximately 6% to current sea level rise (Shepherd and Wingham, 2007) with a potential total contribution of approximately 0.24 m (Vaughan et al., 2006). Strong westerly winds over the Amundsen Sea were shown in the modelling study of Thoma et al. (2008) to divert relatively warm ocean currents onto the continental shelf (i.e. toward the ASE) below floating ice shelves at the base of the glaciers. Melting of these ice shelves could reduce the latitudinal stress on the glacier and explain at least some of the observed acceleration. However, atmospheric circulation over the Amundsen Sea has not been extensively studied due to a lack of long-term in-situ observational records. Recent work has focussed on temperatures over the adjacent West Antarctica (*Ding et al.*, 2011) and shown that tropical Pacific SST anomalies can affect atmospheric circulation over the Amundsen Sea. However, a direct assessment of the westerly winds adjacent to the ACE has not been conducted. The key question addressed here is whether increases in westerly winds have occurred over the Amundsen Sea that might ultimately contribute to the acceleration of the glaciers in the ASE.

The climatological mean winds over the Amundsen Sea exhibit a distinct seasonal cycle with more pronounced westerly winds during the winter and spring seasons (Thoma et al., 2008). This occurs in association with the movement of a climatological centre of low pressure, known as the Amundsen Sea Low, which moves zonally along ~70°S to be situated just east of the Amundsen Sea in summer and over Ross Sea in other months. In any given season there can be large departures from climatology, since the Amundsen Sea is a region of particularly large mean sea-level pressure (MSLP) variability (Cullather et al., 1996; Lachlan-Cope and Connolley, 2003).

As a consequence of the lack of long-term in-situ observational data in the region the main source of data for studying atmospheric circulation over the Amundsen Sea is reanalysis datasets. Reanalyses compensate for the lack of in-situ data by using a wide range of observational data to constrain a full-physics atmospheric model, which provides a best estimate of the real full three-dimensional structure of the atmosphere through time. Satellite retrieved soundings are the most important source of data in regions of sparse in-situ observations, since they can be used to attain relatively accurate estimates of, for example, atmospheric temperature. Here three new reanalyses are assessed (CFSR, ERA-Interim and MERRA) alongside three more established reanalyses (ERA-40, JRA-25 and NNR1), see Table 1 for full names and other details. MSLP data from buoys deployed in the Bellingshausen Sea in late summer/autumn 2001 are used to assess their skill. King (2003) used this buoy dataset in an assessment of ECMWF operational weather analyses since it is an independent dataset that is not assimilated into analyses.

An important motivation for verifying the reanalyses is to determine the best choice of dataset for forcing ocean models in this region. An advantage of assessing a large number of reanalyses is that a measure of confidence in their output can be gained from the inter-model spread. Agreement between the models implies that their output is not sensitive to their different model structures and assimilation schemes.

This paper is structured as follows. In section 2 the reanalysis and drifter buoy datasets are described. The results of the comparison between the reanalyses and buoy data are then presented in section 3. In section 4 the climatology of the westerly geostrophic winds over the Amundsen Sea is shown in detail followed by an assessment of trends and links with the

Southern Annular Mode (SAM) and El Nino-Southern Oscillation (ENSO) in section 5. This is followed by the discussion and conclusions in section 6.

2. Data and methods

Six reanalysis datasets were considered in this assessment: CFSR, ERA-40, ERA-Interim, JRA-25, MERRA and NNR1. Their full names and other details are shown in Table 1. Reanalyses are atmospheric datasets constructed using a weather model to fill the gaps in space and time between in-situ observations.

NNR1, ERA-40 and JRA-25 have been available for a number of years. Bromwich et al. (2007) provide a comprehensive review of the performance of these more established reanalyses over the polar regions. They exhibit large biases in the Southern Hemisphere troposphere before the widespread introduction of satellite-retrieved soundings in 1979 (Hines et al. 2000; Marshall and Harangozo, 2000; Renwick, 2004; Sterl, 2004). In the modern satellite era (i.e. since 1979) NNR1 showed significant biases in mean MSLP around Antarctica persisting into the 1990s. This was due to observations being rejected where differences from the model were large. Since 1979 a steady increase in the number of in-situ observations and upgrades/additions to satellite-borne remote sensing has resulted in an increase in the number of accepted observations. In particular many Australian automatic weather stations were assimilated in the mid 1990s, which was probably the main contributor in ending an MSLP bias in NNR1 over East Antarctica (Hines et al., 2000; Marshall and Harangozo, 2000; Bromwich and Fogt, 2004). ERA-40 shows consistently small biases in MSLP after 1979 when compared to in-situ observational records. Bromwich et al. (2007) found better agreement between JRA-25 and ERA-40 than between NNR1 and ERA-40, indicating that JRA-25 biases are also relatively small during the modern satellite era. Differences in SLP between all three are relatively small over the Amundsen Sea region (Bromwich et al., 2007).

Anomalies in the stratosphere are now recognised as having an impact on surface atmospheric circulation (Thompson et al., 2005). Comparisons with observations in the stratosphere over the poles are more difficult due to the lack of in-situ measurements. The most detailed assessments are based on superpressure balloon campaigns such as those of *Manney et al.* (2005) and *Boccara et al.* (2008). As with the troposphere they find that ERA-40 is more accurate than NNR1, but do not assess JRA-25.

In recent years a new generation of reanalyses have been launched (MERRA, ERA-Interim and CFSR). Their skill in simulating Antarctic climate is not yet well known. Some of the important aspirations/improvements are: (i) increased resolution, (ii) improved observational datasets, (iii) more realistic representation of stratospheric dynamics (iv) improved assimilation and bias correction of satellite radiances and (v) improved representations of the hydrological cycle. It is notable that a 4D-Var data assimilation scheme is used in ERA-Interim, which would be expected to incorporate the observational data in a more dynamically consistent way than the 3D-Var schemes used in the other reanalyses. More details can be found in the references listed in Table 1. It should also be noted that MERRA and CFSR share common origins. In particular both the input data and analysis system used for MERRA and CFSR are nearly the same (Saha et al., 2010).

A dataset of MSLP measurements from drifting buoys deployed on sea ice in the Bellingshausen Sea was used to compare the skill of the reanalysis datasets off coastal West Antarctica. Since the Bellingshausen Sea is located only 500 km to the east of the Amundsen Sea, this dataset should give a good indication of the performance of the reanalyses over the Amundsen Sea. The MSLP dataset comprises data from three Metocean Compact Air-Launched

Ice Drifters (CALIBs) and intermittently spans the period 18 February to 21 May 2001. The Global Telecommunications System (GTS) of the World Meteorological Organization (WMO) did not have access to the data, which are therefore an independent source of information as they were not assimilated into atmospheric analyses. From a deployment of three CALIBs on 18 February one failed shortly after but the other two (ARGOS IDs 21376 and 21388) were successful. Another CALIB was deployed on 25 April (ARGOS ID 21392). However, King (2003) points out that just after the deployment of CALIB 21392 three surface velocity profiling barometers (SVPBs) were deployed approximately 135 km to the north and sent data to the GTS. Therefore the approach of King (2003) is followed by focussing on data from CALIBs 21376 and 21388 over the period that they produced reliable data from 18 February through 15 March. For more details of the CALIB dataset including a map of buoy locations see King (2003).

For comparisons between reanalysis and observations, the CALIB observations made at the model analysis times 00, 06, 12 and 18Z ± 1 hour were selected. A bilinear interpolation was then used to extract MSLP from the gridded reanalyses at the CALIB locations. Where more than one MSLP observation from a given CALIB occurs within 1 hour of one of the analysis times, an average of these observations was used.

3. Comparison between reanalyses and drifting buoy observations

Following King (2003) interpolated reanalysis data are compared to CALIBs 21376 and 21388 over the period 18 February through 15 March 2001 (Figure 1). From Figure 1 it is clear that most of the reanalyses agree well with the CALIB data. However, relatively large differences of ~5-10 hPa occur frequently for the JRA-25 and NNR1 reanalyses. JRA-25 also exhibits a dependence on pressure, with larger positive biases for lower pressure, which indicates particular problems with simulating cyclones. Such dependence is not evident for the other reanalyses. The mean bias and variance (standard deviation) of the differences are plotted in Figure 2a shows that in most cases the mean bias is within or very close to the CALIB instrumental error of 1 hPa. The exceptions are the positive mean biases seen in NNR1 (CALIBs 21376 and 21388) and JRA-25 (CALIB 21388). The MSLP biases in NNR1 have been well documented in previous studies (e.g. Bromwich and Fogt, 2004; Marshall, 2003). However, the reason for particularly large differences between JRA-25 and 23188 is not clear. However, comparing the different reanalyses over many years shows distinct year-to-year variations in the relative biases over the Bellingshausen Sea (Figure 3). The slightly larger mean bias in JRA-25 compared to the other reanalyses over the period spanned by the CALIB data cannot be taken as representative of the full period since 1979. Indeed it is clear from Figure 3 that, apart from NNR1, there is generally good agreement between the reanalyses.

The variance about the mean bias shows clearer differences between different reanalyses (Figure 2). ERA-Interim shows the smallest variance, which indicates that it is the most accurate at simulating specific weather events such as cyclones and fronts. ERA-40 shows the next smallest variance, despite having a lower spatial resolution than MERRA and CFSR. This is possibly an indication that ERA-40 makes better use of available observations to constrain the model. NNR1 shows the largest variance . Only ERA-Interim matches the performance of the ECMWF operational model that was the subject of analysis of King (2003).

For a short period CALIBs 21376 and 21388 were transmitting simultaneously. Therefore the MSLP gradient between them could be compared with the reanalyses. Figure 2b shows differences between the gradients recorded by the CALIBs and those extracted from reanalysis data. It is difficult to draw robust conclusions from this, since the model-CALIB differences are mainly less than the cumulative instrumental error from the two CALIBs (2 hPa).

Results from just one or two months are of course unlikely to be fully representative of the longer-term performance of the reanalysis datasets. For instance the skill can vary with season. There may also be variations across models in their skill at simulating specific weather patterns such as blocking, which can vary in prevalence over a one-month time scale.

The relative differences between the reanalyses in MSLP estimates over the Amundsen Sea are very similar to those seen over the Bellingshausen Sea (Figure 3). This shows that the general good agreement between the CALIB data and reanalyses over the Bellinghausen Sea is a good indication of skill over the Amundsen Sea.

4. Geostrophic wind climatology and variability

There is a distinct seasonal variation of the MSLP pattern over the Amundsen Sea. During most of the year a climatological centre of low pressure (the Amundsen Sea Low) is located towards the Ross Sea. However, during summer the Amundsen Sea Low moves to the east towards the Bellingshausen Sea. Thoma et al. (2008) show that over the Amundsen Sea this gives mainly westerly geostrophic winds for most of the year, with a period of weak easterlies in summer. They use a westerly geostrophic wind index to capture this variability, which is the difference between the mean along two latitudinal arcs at 67.5°S and 72.5°S. Both arcs span the longitude range 100°W to 125°W. The region over which this is defined in indicated in Figure 4a. Here the index is denoted as Δp_{AS}. A positive index therefore indicates westerly geostrophic wind (a Δp_{AS} of 1 hPa corresponds to a geostrophic westerly wind of ~2 ms^{-1}).

The annual mean climatology of MSLP as estimated from ERA-Interim is shown in Figure 4a. This shows that the long-term mean annual average gives very weak MSLP gradients over the

Amundsen Sea. ERA-Interim was chosen due to its greater accuracy compared to the CALIB data. CFSR and MERRA also span the full period from 1979. Climatological differences between ERA-Interim and CFSR over this period are generally small away from land, as demonstrated by Figure 4b. However, the differences do indicate a slightly more positive Δp_{AS} in ERA-Interim compared to CFSR. Almost identical differences were found between ERA-Interim and MERRA (not shown). Larger differences become apparent over West Antarctica, but MSLP is not a valid quantity over high elevations.

The rather stagnant annual average MSLP gradient is not representative of the majority of months, or indeed seasons. A time series showing Δp_{AS} from 1979 through 2009 filtered to seasonal (3-month) time scales shows the clear intra-annual fluctuations between westerly and easterly near-surface winds (Figure 5). It is the periods of strong positive Δp_{AS} that have been found to coincide with intrusions of circumpolar deep water onto the continental shelf toward the ASE (Thoma et al., 2008). The different reanalyses generally show similar results and it is difficult to distinguish between them in Figure 5.

The inter-model differences are more apparent with a twelve-month low-pass filter applied to the Δp_{AS} time series (Figure 6). The differences between the reanalyses are largest during the 1980s and reduce during the 1990s, in agreement with the idea that additions and improvements in the observations have gradually reduced biases over the modern satellite era (Bromwich et al., 2007). The position of each model in the inter-model range remains broadly constant over time. For instance, during most of the period JRA-25 is at or near the top of the inter-model range and NNR1 is at or near the bottom. From year to year however the relative bias among the models changes quite markedly. The changes in bias over time are important when considering long-term trends. The reanalyses that span the full period clearly show more positive values of Δp_{AS} from the early 1990s onwards, with a large change at approximately 1992. It is unlikely that this large change is an artefact of changes in observational input data. Previous studies have identified such artefacts in a number of reanalyses, but not for the year 1992 (Onogi et al., 2007; Sakamoto and Christy, 2009; Bromwich et al., 2011; Screen and Simmonds, 2011). In addition these studies show that in general reanalyses systems respond differently to changes in input data, further suggesting that the change in 1992 is not an artefact. The reliability of this increase in Δp_{AS} will be discussed in the context of the SAM in the next section.

5. Recent trends and links with large-scale variability

In order to assess long-term changes over the Amundsen Sea it is important to determine links with larger scale weather patterns. If robust links are identified then it can be possible to link regional change to factors such as the ozone hole (Marshall et al., 2006). The possibility of developing an ice-core proxy for Δp_{AS} is also an important motivation for assessing large-scale links. Of the four most recent reanalyses, CFSR, ERA-Interim and MERRA were used for assessing variability. The other, JRA-25, was not used since it produces mean biases larger than instrumental error (Figure 2) and shows and a strong dependence between bias and pressure (Figure 1).

Month-to-month variability in Δp_{AS} estimated from ERA-Interim is strongly positively correlated with MSLP variability over the South Pacific sector of the Southern Ocean, with a maximum of 0.7 at approximately 62°S, 120°W (Figure 7). Somewhat weaker negative correlations of between -0.2 and -0.4 extend over all Antarctica. A ring of small positive correlations at ~40°S indicates only a weak positive correlation with the SAM index. The results from CFSR and MERRA data are almost identical (not shown).

Time series of annual mean Δp_{AS} calculated from CFSR, ERA-Interim and MERRA are shown in Figure 8 along with the SAM index of Marshall (2003), which is based entirely on long-term in-situ observations. For the purposes of comparison with the SAM index the Δp_{AS} time series are normalised by their standard deviation. There is little correspondence between Δp_{AS} and the SAM index in terms of year-to-year variability (r=0.00 for ERA-Interim). However, a change from lower SAM index values in the 1980s to higher values since the early 1990s broadly correlates with the decadal changes in Δp_{AS} seen in the reanalysis datasets (Figure 6).

If the trends in the SAM are indeed linked to the trends in Δp_{AS} then one would expect a strong seasonal dependence in the trends in Δp_{AS} that matches the well-documented seasonal dependence of trends in the SAM (Thompson and Solomon, 2002). The summer (December-February) and autumn (March-May) trends in Δp_{AS} are much more strongly positive and follow the decadal changes in the SAM (Figure 9). Both indices show a rapid summer and autumn increase from the mid 1980s to ~2000 after which they return to more neutral values. The correlations are only significant ($p \leq 0.05$) in summer. For winter there is no correlation between the SAM and Δp_{AS} (r=0.01 for both CFSR and MERRA and r=-0.00 for ERA-Int) and neither index shows a detectable linear trend (Figure 9).

In addition to correlations with the SAM, previous studies indicate relatively strong correlations between ENSO and pressures over the Amundsen Sea of up to 0.5 in winter (e.g. Harangozo, 2000). The correlation between Δp_{AS} estimated from ERA-Interim and the NINO3.4 index in winter is 0.24, which is comparatively weak. A much stronger correlation coefficient of 0.41 (significant for $p \leq 0.05$) is found for spring (Figure 10) and a much weaker correlation of 0.17 (insignificant for $p > 0.05$) in both summer and autumn. Calculations based on CFSR and MERRA gives almost identical correlation coefficients.

6. Discussion and conclusions

In this paper the climatology and variability of westerly geostrophic wind over the Amundsen Sea has been documented. This is potentially an important factor in affecting the melt rate at the base of ice shelves that flow out from glaciers into the Amundsen Sea (Thoma et al., 2008).

There are no long-term in-situ observational records over the Amundsen Sea or the surrounding region. Reanalysis datasets were therefore the main source of meteorological data used in this study. Three new reanalyses (CFSR, ERA-Interim and MERRA) were assessed alongside three more established reanalyses (ERA-40, JRA-25 and NNR1). A comparison with independent mean sea level pressure (MSLP) data from ice drifting buoys (CALIBs) showed that ERA-Interim is clearly the most accurate over the neighbouring Bellingshausen Sea, implying that it is also accurate over the Amundsen Sea. Other reanalyses were found to be less accurate (i.e. larger bias variances), but in almost all cases showed mean biases within the CALIB instrumental error. This implies that relative to ERA-Interim the other reanalyses are not as successful at capturing the details of individual weather systems, but with the exception of NNR1 produce a similarly accurate mean state. CFSR, ERA-Interim and MERRA were used for the correlation analysis back to 1979. JRA-25 was not used since it showed a larger bias variance than the other reanalyses and a strong dependence between bias and pressure.

Strong westerly winds over the Amundsen Sea are associated with a distinct high-pressure ridge that is centred at the same longitude as the Amundsen Sea and just north of 60°S (Figure 7). This is consistent with the case study of strong westerly winds conducted by Thoma et al. (2008), which shows a high pressure ridge in the same location in spring 1994. The strong correlation with pressures over the extreme South Pacific is probably the reason for the positive correlation with ENSO (NINO3.4), which is strongest (0.41; $p \leq 0.05$) in the spring season.

Year-to-year correlations between Δp_{AS} and the SAM are much smaller, but trends in both indices follow the same decadal pattern and seasonal dependence. This indicates that an external underlying factor (or a number of factors) influences the decadal changes in both. Modelling studies show strong evidence that the annual cycle in the SAM trends can be explained by the formation of the ozone hole, the effect of which propagates down from the stratosphere to affect the troposphere in winter and autumn (Thompson and Solomon, 2002). It is possible that in addition to projecting on the SAM (i.e. increasing the strength of the circumpolar westerly winds over the Southern Ocean), the westerly winds over the Amundsen Sea are also affected by the ozone hole. The wider implication of the positive trends in Δp_{AS} is that there are ongoing changes that act to increase the frequency/severity of intrusions of circumpolar deep water to the inner continental shelf of the Amundsen Sea. Thoma et al. (2008) forced their ocean model using NNR1 and found a decade of warming of shelf water in the 1990s. Our results show that the increase in Δp_{AS}, to which this warming was attributed, is robustly reproduced by other reanalyses. The close correspondence to decadal changes in the SAM further suggests that these changes are not merely an artefact of the reanalysis models.

A number of questions remain for future work. How did Δp_{AS} vary before 1979 and can we use ice core proxies to determine this? To what extent have climate drivers such as the ozone hole, greenhouse gases and volcanic eruptions contributed to changes in Δp_{AS} and are any climate models sufficiently reliable in their simulation of the Amundsen Sea region to answer this question? Are the changes in Δp_{AS} documented here large enough to have a significant impact on ocean temperatures, hence on melting of ice shelves, hence on the flow speed of glaciers?

Acknowledgements

Thanks to Paul Holland and one anonymous reviewer for their comments, which greatly helped to improve the manuscript. This study is part of the British Antarctic Survey Polar Science for Planet Earth Programme. It was funded by UK The Natural Environment Research Council. The European Centre for Medium Range Weather Forecasting are thanked for providing the ERA-40 and ERA-Interim datasets. The JRA-25 dataset used for this study was provided from the cooperative research project of the JRA-25 long-term reanalysis by the Japan Meteorological Agency (JMA) and the Central Research Institute of Electric Power Industry (CRIEPI). The Global Modeling and Assimilation Office (GMAO) and the GES DISC are acknowledged for the dissemination of the MERRA dataset. The CFSR data was retrieved from the Research Data Archive, which is managed by the Data Support Section of the Computational and Information Systems Laboratory at the National Center for Atmospheric Research in Boulder, Colorado. The NNR1 Reanalysis Derived data was provided by the NOAA/OAR/ESRL PSD, Boulder, Colorado, USA, from their Web site at http://www.esrl.noaa.gov/psd/.

Bibliography

Boccara G, Hertzog A, Basdevant C, Vial F. 2008. Accuracy of NCEP/NCAR reanalyses and ECMWF analyses in the lower stratosphere over Antarctica in 2005. *Journal of Geophysical Research-Atmospheres*. **113**(D20). 10.1029/2008jd010116.

Bromwich DH, Fogt RL. 2004. Strong Trends in the Skill of the ERA-40 and NCEP-NCAR Reanalyses in the High and Midlatitudes of the Southern Hemisphere, 1958-2001. *Journal of Climate*. **17**(23): 4603-4619. 10.1175/3241.1.

Bromwich DH, Nicolas JP, Monaghan AJ. 2011. An Assessment of Precipitation Changes over Antarctica and the Southern Ocean since 1989 in Contemporary Global Reanalyses. *Journal of Climate*. **24**(16): 4189-4209. 10.1175/2011jcli4074.1.

Bromwich DH, Fogt RL, Hodges KI, Walsh JE (2007), A tropospheric assessment of the ERA-40, NCEP, and JRA-25 global reanalyses in the polar regions, *Journal of Geophysical Research-Atmospheres, 112*(D10), D10111, doi: 10.1029/2006jd007859.

Cullather RI, Bromwich DH, Van Woert ML. 1996. Interannual variations in Antarctic precipitation related to El Nino southern oscillation. *Journal of Geophysical Research*. **101**: 19109-19118.

Dee DP, Uppala SM, Simmons AJ, Berrisford P, Poli P, Kobayashi S, Andrae U, Balmaseda MA, Balsamo G, Bauer P, Bechtold P, Beljaars ACM, van de Berg L, Bidlot J, Bormann N, Delsol C, Dragani R, Fuentes M, Geer AJ, Haimberger L, Healy SB, Hersbach H, Holm EV, Isaksen L, Kallberg P, Kohler M, Matricardi M, McNally AP, Monge-Sanz BM, Morcrette JJ, Park BK, Peubey C, de Rosnay P, Tavolato C, Thepaut JN, Vitart F. 2011. The ERA-Interim reanalysis: configuration and performance of the data assimilation system. *Quarterly Journal of the Royal Meteorological Society*. **137**(656): 553-597. 10.1002/qj.828.

Ding Q, Steig EJ, Battisti DS, Kuttel M. 2011. Winter warming in West Antarctica caused by central tropical Pacific warming. *Nature Geoscience*. **4**(6): 398-403. 10.1038/ngeo1129.

Harangozo SA. 2000. A search for ENSO teleconnections in the west Antarctic Peninsula climate in Austral winter. *International Journal of Climatology*. **20**: 663-679.

Hines KM, Bromwich DH, Marshall GJ. 2000. Artificial surface pressure trends in the NCEP/NCAR reanalysis over the Southern Ocean and Antarctica. *Journal of Climate*. **12**: 3940-3952. 10.1175/1520-0442(2000)013<3940:ASPTIT>2.0.CO;2.

Kalnay E, Kanamitsu M, Kistler R, Collins W, Deaven D, Gandin L, Iredell M, Saha S, White G, Woollen J, Zhu Y, Chelliah M, Ebisuzaki W, Higgins W, Janowiak J, Mo KC, Ropelewski C, Wang J, Leetmaa A, Reynolds R, Jenne R, Joseph D. 1996. The NCEP/NCAR 40-year reanalysis project. *Bulletin of the American Meteorological Society*. **77**: 437-471.

King JC. 2003. Validation of ECMWF sea level pressure analyses over the Bellingshausen Sea, Antarctica. *Weather and Forecasting*. **18**: 536-540.

Lachlan-Cope T, Connolley W. 2006. Teleconnections between the tropical pacific and the amundsen-bellinghausens sea: Role of the El Nino Southern Oscillation. *Journal of Geophysical Research-Atmospheres*. **111**(D23). 10.1029/2005jd006386.

Manney GL, Allen DR, Kruger K, Naujokat B, Santee ML, Sabutis JL, Pawson S, Swinbank R, Randall CE, Simmons AJ, Long C. 2005. Diagnostic comparison of meteorological analyses during the 2002 antarctic winter. *Monthly Weather Review*. **133**(5): 1261-1278. 10.1175/MWR2926.1.

Marshall GJ. 2003. Trends in the Southern Annular Mode from observations and reanalyses. *Journal of Climate*. **16**: 4134-4143.

Marshall GJ, Harangozo SA. 2000. An appraisal of NCEP/NCAR reanalysis MSLP viability for climate studies in the South Pacific. *Geophysical Research Letters*. **27**: 3057-3060.

Marshall GJ, Orr A, van Lipzig NPM, King JC. 2006. The impact of a changing Southern Hemisphere Annular Mode on Antarctic Peninsula summer temperatures. *Journal of Climate*. **19**(20): 5388-5404.

Onogi K, Tslttsui J, Koide H, Sakamoto M, Kobayashi S, Hatsushika H, Matsumoto T, Yamazaki N, Kaalhori H, Takahashi K, Kadokura S, Wada K, Kato K, Oyama R, Ose T, Mannoji N, Taira R. 2007. The JRA-25 reanalysis. *Journal of the Meteorological Society of Japan*. **85**(3): 369-432. 10.2151/jmsj.85.369.

Renwick JA. 2004. Trends in the Southern Hemisphere polar vortex in NCEP and ECMWF reanalyses. *Geophysical Research Letters*. **31**: L07209-L07207doi.

Rienecker MM, Suarez MJ, Gelaro R, Todling R, Bacmeister J, Liu E, Bosilovich MG, Schubert SD, Takacs L, Kim G-K, Bloom S, Chen J, Collins D, Conaty A, Da Silva A, Gu W, Joiner J, Koster RD, Lucchesi R, Molod A, Owens T, Pawson S, Pegion P, Redder CR, Reichle R, Robertson FR, Ruddick AG, Sienkiewicz M, Woollen J. 2011. MERRA: NASA's Modern-Era Retrospective Analysis for Research and Applications. *Journal of Climate*. **24**(14): 3624-3648. 10.1175/jcli-d-11-00015.1.

Rignot E, Bamber JL, Van Den Broeke MR, Davis C, Li YH, Van De Berg WJ, Van Meijgaard E. 2008. Recent Antarctic ice mass loss from radar interferometry and regional climate modelling. *Nature Geoscience*. **1**(2): 106-110. 10.1038/ngeo102.

Saha S, Moorthi S, Pan HL, Wu XR, Wang JD, Nadiga S, Tripp P, Kistler R, Woollen J, Behringer D, Liu HX, Stokes D, Grumbine R, Gayno G, Wang J, Hou YT, Chuang HY, Juang HMH, Sela J, Iredell M, Treadon R, Kleist D, Van Delst P, Keyser D, Derber J, Ek M, Meng J, Wei HL, Yang RQ, Lord S, Van den Dool H, Kumar A, Wang WQ, Long C, Chelliah M, Xue Y, Huang BY, Schemm JK, Ebisuzaki W, Lin R, Xie PP, Chen MY, Zhou ST, Higgins W, Zou CZ, Liu QH, Chen Y, Han Y, Cucurull L, Reynolds RW, Rutledge G, Goldberg M. 2010. The NCEP Climate Forecast System Reanalysis. *Bulletin of the American Meteorological Society*. **91**(8): 1015-1057. 10.1175/2010bams3001.1.

Sakamoto M, Christy JR. 2009. The Influences of TOVS Radiance Assimilation on Temperature and Moisture Tendencies in JRA-25 and ERA-40. *Journal of Atmospheric and Oceanic Technology*. **26**(8): 1435-1455. 10.1175/2009jtecha1193.1.

Screen JA, Simmonds I. 2011. Erroneous Arctic Temperature Trends in the ERA-40 Reanalysis: A Closer Look. *Journal of Climate*. **24**(10): 2620-2627. 10.1175/2010jcli4054.1.

Shepherd A, Wingham D. 2007. Recent sea-level contributions of the Antarctic and Greenland ice sheets. *Science*. **315**(5818): 1529-1532. 10.1126/science.1136776.

Shepherd A, Wingham DJ, Mansley JAD, Corr HFJ. 2001. Inland thinning of Pine Island Glacier, West Antarctica. *Science*. **291**(5505): 862-864.

Sterl A. 2004. On the (in)homogeneity of reanalysis products. *Journal of Climate*. **17**(19): 3866-3873.

Thoma M, Jenkins A, Holland D, Jacobs S. 2008. Modelling Circumpolar Deep Water intrusions on the Amundsen Sea continental shelf, Antarctica. *Geophysical Research Letters*. **35**(18). 10.1029/2008gl034939.

Thompson DWJ, Solomon S (2002), Interpretation of recent Southern Hemisphere climate change, *Science*, *296*, 895-899, doi: 10.1126/science.1069270.

Thompson DWJ, Baldwin MP, Solomon S. 2005. Stratosphere-troposphere coupling in the Southern Hemisphere. *Journal of the Atmospheric Sciences*. **62**(3): 708-715.

Uppala SM, Kallberg PW, Simmons AJ, Andrae U, Bechtold VD, Fiorino M, Gibson JK, Haseler J, Hernandez A, Kelly GA, Li X, Onogi K, Saarinen S, Sokka N, Allan RP, Andersson E, Arpe K, Balmaseda MA, Beljaars ACM, van de Berg L, Bidlot J, Bormann N, Caires S, Chevallier F, Dethof A, Dragosavac M, Fisher M, Fuentes M, Hagemann S, Holm E, Hoskins BJ, Isaksen L, Janssen PAEM, Jenne R, McNally AP, Mahfouf JF, Morcrette JJ, Rayner NA, Saunders RW, Simon P, Sterl A, Trenberth KE, Untch A, Vasiljevic D, Viterbo P, Woollen J (2005), The ERA-40 re-analysis, *Quarterly Journal of the Royal Meteorological Society*, *131*, 2961-3012, doi: 10.1256/qj.04.176.

Vaughan DG, Corr HFJ, Ferraccioli F, Frearson N, O'Hare A, Mach D, Holt JW, Blankenship DD, Morse DL, Young DA. 2006. New boundary conditions for the West Antarctic Ice sheet: Subglacial topography beneath Pine Island Glacier. *Geophysical Research Letters*. **33**(9). 10.1029/2005gl025588.

Figure captions

Figure 1. CALIBs 21376 and 21388 compared to CFSR, ERA-40, ERA-Interim, JRA-25 MERRA and NNR1.

Figure 2. Differences between reanalyses (which are grouped as labelled along the abscissa) and CALIB data. (left panel) For all CALIB data (90, 50 and 100 obs for CALIBs 21376, 21388 and 21392 respectively) and (right panel) for differences between simultaneous data points from CALIB 21376 and 21388 (46 obs). The mean reanalysis minus CALIB differences are shown by the symbol and the bars show the standard deviations. The different symbols in (a) denote different CALIBs as indicated in the key. The dotted lines show the instrumental error. In (b) a cumulative instrumental error was used since no information on the statistical distribution of instrumental errors was available.

Figure 3. Sea-level pressure from reanalyses for (left) the Bellingshausen Sea (72.5S, 90W) and (right) the Amundsen Sea (72.5S, 110W). A one-year low pass digital filter was applied to the time series of monthly mean data.

Figure 4. (a) ERA-Interim climatological annual mean MSLP for 1979-2009. (b) The difference in climatological annual mean MSLP between ERA-Interim and CFSR for 1979-2009. The region over which Δp_{AS} is defined is indicated by the box in (a) and the location of the Amundsen Sea Embayment is indicated by 'ASE'.

Figure 5. Seasonal timescale variations of time series of the Amundsen Sea SLP index from the various reanalysis datasets. The monthly data was smoothed using a low pass (3-month threshold) digital filter.

Figure 6. Annual timescale variations of time series of the Amundsen Sea SLP index from the various reanalysis datasets. The monthly data was smoothed using a low pass (12-month threshold) digital filter.

Figure 7. The spatial distribution of correlations between time series of monthly mean MSLP at all grid points and the time series of monthly mean Δp_{AS}. Prior to calculating correlations all time series were processed as follows: (i) the multi-year mean for each month was subtracted, (ii) each calendar month was normalised by the standard deviation of the year-to-year variability for that month and (iii) a linear detrending was applied. The bold black line shows the contour for a p-value of 0.05. Data from ERA-Interim.

Figure 8. The Marshall SAM index (solid line) and normalised Δp_{AS} (dashed line:CFSR, dashed-dot line: MERRA, dashed-dot-dot-dot line: ERA-Interim). The time series of annual mean Δp_{AS} was normalised by the standard deviation of its year-to-year variability. The correlation coefficient between the Marshall index and Δp_{AS} from ERA-Interim (both linearly detrended) is shown in the plot title.

Figure 9. As in Figure 8 but for summer (DJF), autumn (MAM), winter (JJA) and spring (SON). In each season the time series of Δp_{AS} was normalised by the standard deviation of its year-to-year variability in that season. For DJF the year refers to December. The correlation coefficients between the Marshall index and Δp_{AS} from ERA-Interim (both linearly detrended) are shown in the plot titles.

Figure 10. As for Figure 8, but with Δp_{AS} (dashed line) plotted with NINO3.4 (solid line) in spring (SON). The correlation coefficient between the NINO3.4 index and Δp_{AS} from ERA-Interim (both linearly detrended) is shown in the plot title.

Tables

Table 1. Reanalysis product details.

Name (full name)	Reference	Data period	Horizontal grid (approx. grid size at 50° latitude)	Model top (hPa)
CFSR (NCEP Climate Forecast System Reanalysis)	Saha et al.(2010)	1979-present	T382 (~ 34 km)	~ 0.27
ERA-40 (European Centre for Medium Range Weather Forecasting 40 Year Re-analysis)	Uppala et al. (2005)	September 1957-August 2002	T159 (N80; ~125 km)	0.1
ERA-Interim (European Centre for Medium Range Weather Forecasting Interim Re-analysis)	Dee et al.(2011)	1979-present	T255 (N128; ~79 km)	0.1
JRA-25 (Japanese 25-year Reanalysis)	Onogi et al. (2007)	1979-present	T106 (~120 km)	0.4
MERRA (NASA Modern Era Retrospective-Analysis for Research and Applications)	Rienecker et al. (2011)	1979-present	0.5°×0.67° (~50 km)	0.01
NNR1 (National Centers for Environmental Prediction (NCEP) / NCAR (National Center for Atmospheric Research) Reanalysis 1)	Kalnay et al. (1996)	1948-present	T62 (~210 km)	~ 3

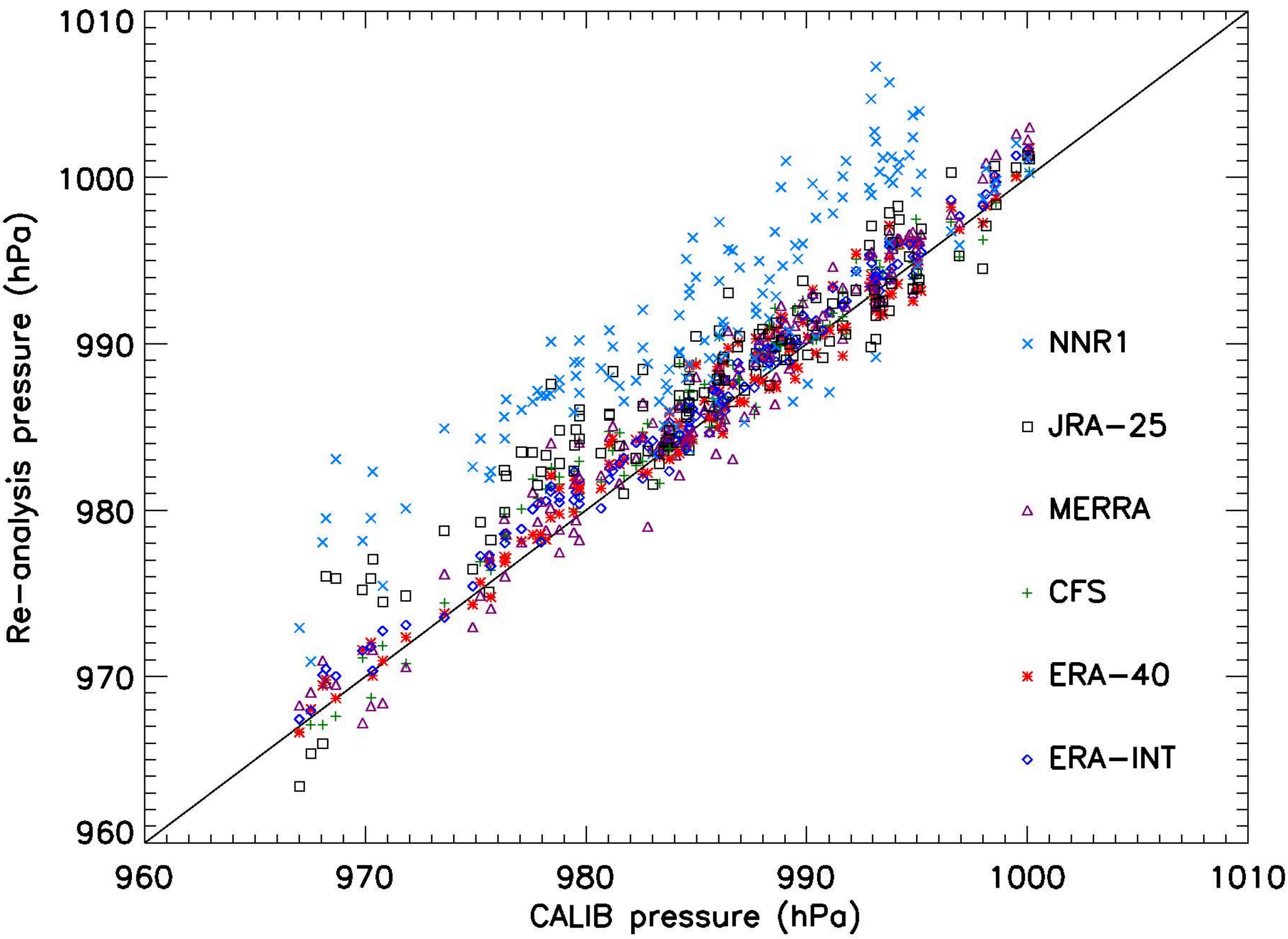
1010
1000
990
980
970
960
960
970
980
990
1000
1010
Re-analysis pressure (hPa)
CALIB pressure (hPa)
NNR1
JRA-25
MERRA
CFS
ERA-40
ERA-INT

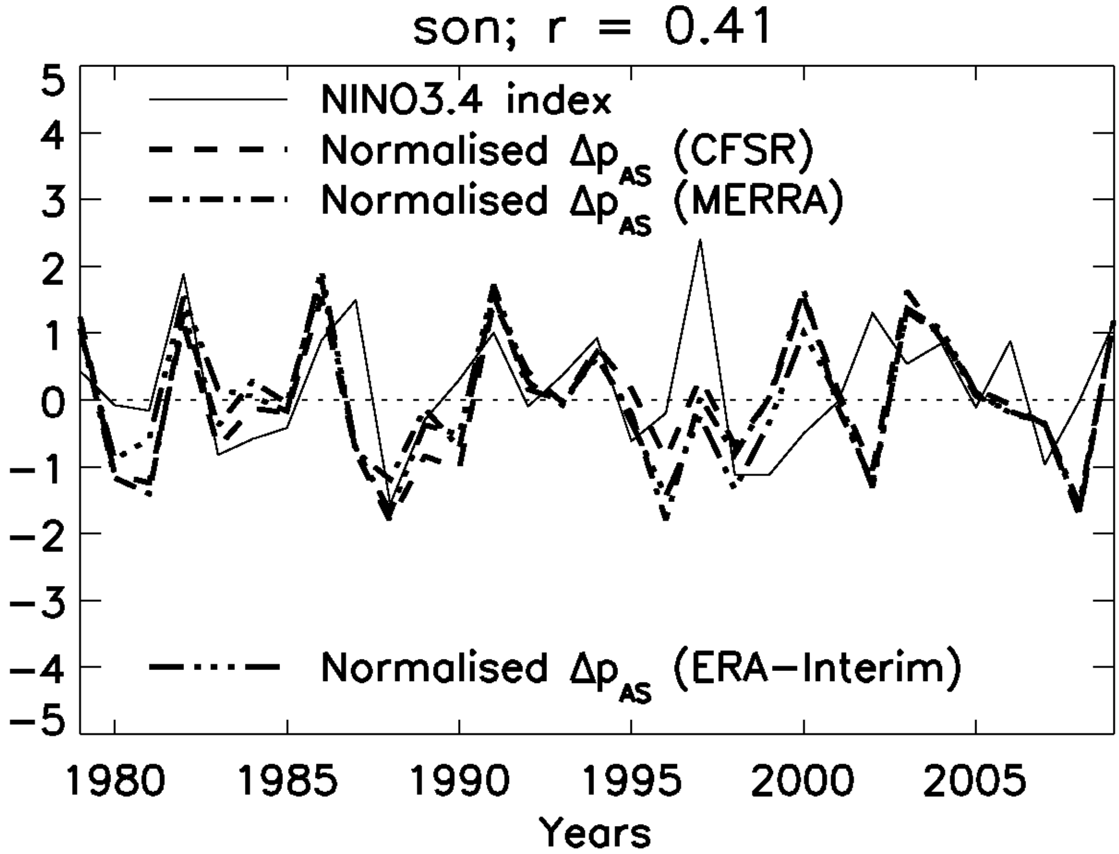

son; r = 0.41
NINO3.4 index
Normalised Δp_AS (CFSR)
Normalised Δp_AS (MERRA)
Normalised Δp_AS (ERA−Interim)
5
4
3
2
1
0
−1
−2
−3
−4
−5
1980
1985
1990
1995
2000
2005
Years

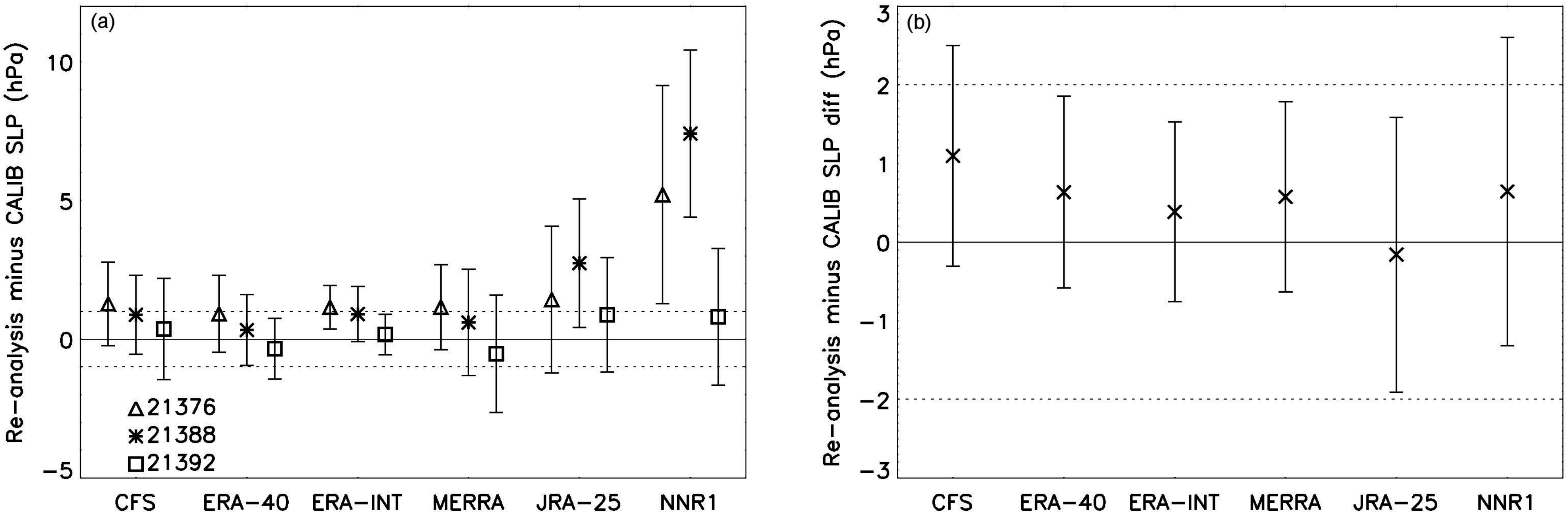
(a)
Re-analysis minus CALIB SLP (hPa)
10
5
0
-5
21376
21388
21392
CFS
ERA-40
ERA-INT
MERRA
JRA-25
NNR1
(b)
Re-analysis minus CALIB SLP diff (hPa)
3
2
1
0
-1
-2
-3
CFS
ERA-40
ERA-INT
MERRA
JRA-25
NNR1

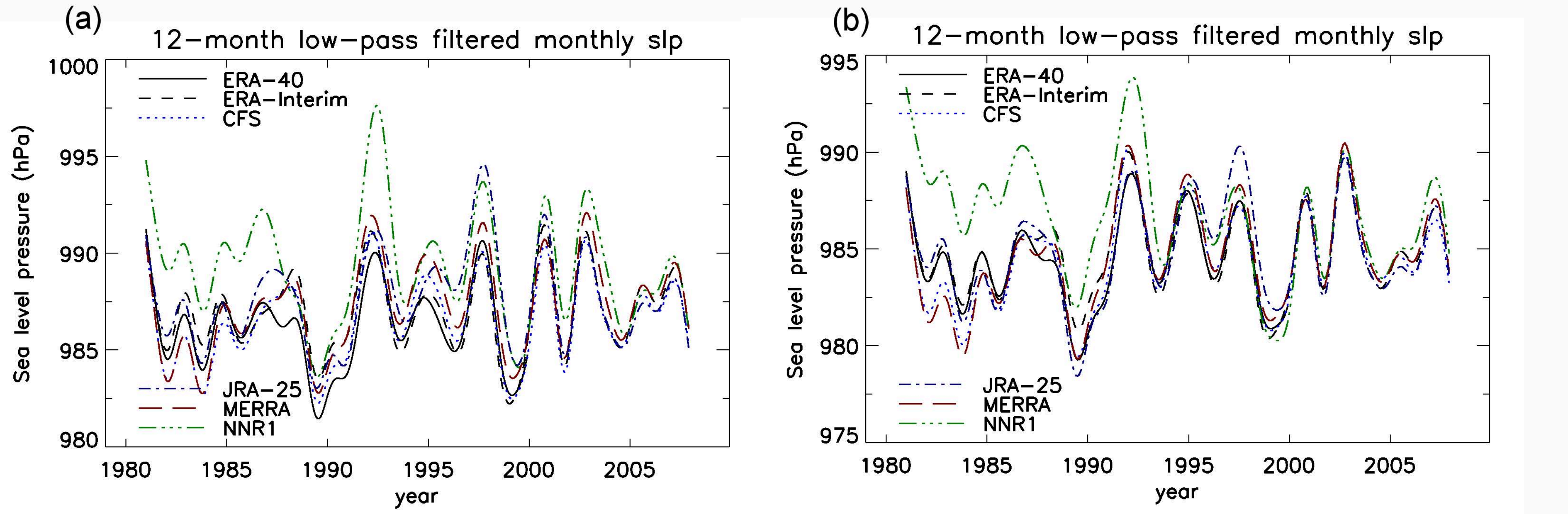
(a)
12-month low-pass filtered monthly slp
Sea level pressure (hPa)
1000
995
990
985
980
1980
1985
1990
1995
2000
2005
year
ERA-40
ERA-Interim
CFS
JRA-25
MERRA
NNR1
(b)
12-month low-pass filtered monthly slp
Sea level pressure (hPa)
995
990
985
980
975
1980
1985
1990
1995
2000
2005
year
ERA-40
ERA-Interim
CFS
JRA-25
MERRA
NNR1

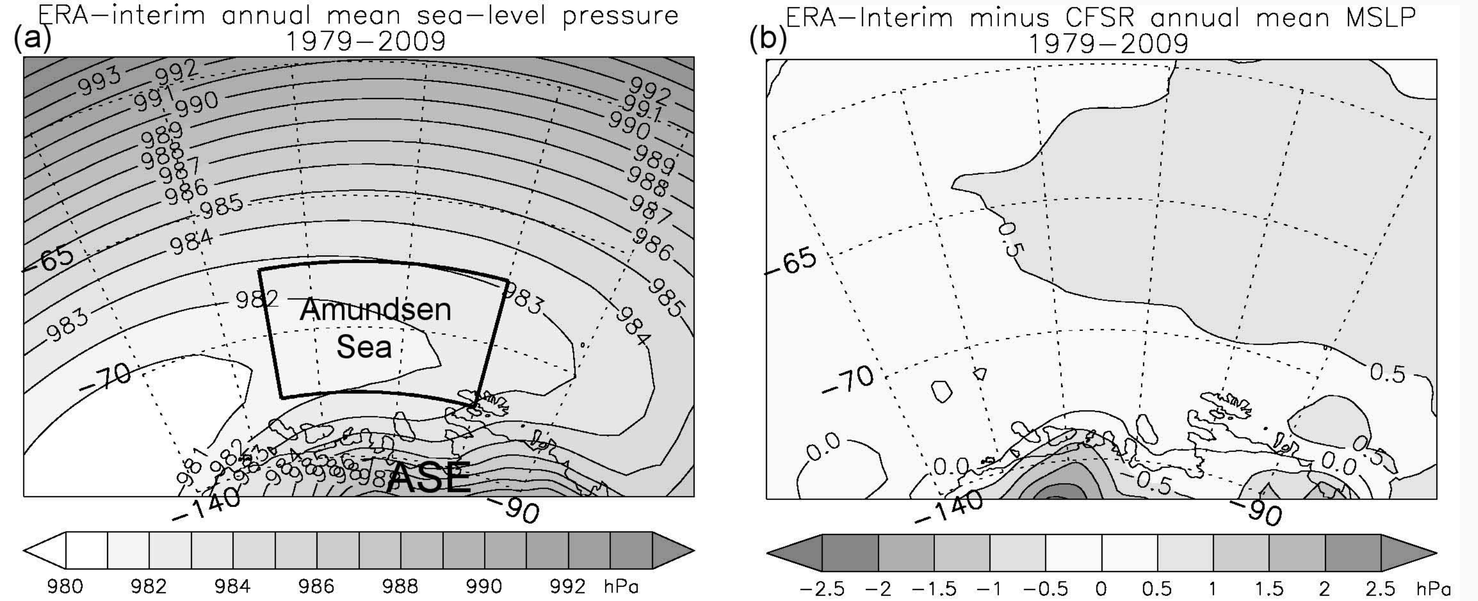
(a)
ERA–interim annual mean sea–level pressure
1979–2009
Amundsen
Sea
ASE
−65
−70
−140
−90
980
982
984
986
988
990
992
hPa
(b)
ERA–Interim minus CFSR annual mean MSLP
1979–2009
−65
−70
−140
−90
0.5
0.0
−2.5
−2
−1.5
−1
−0.5
0
0.5
1
1.5
2
2.5
hPa

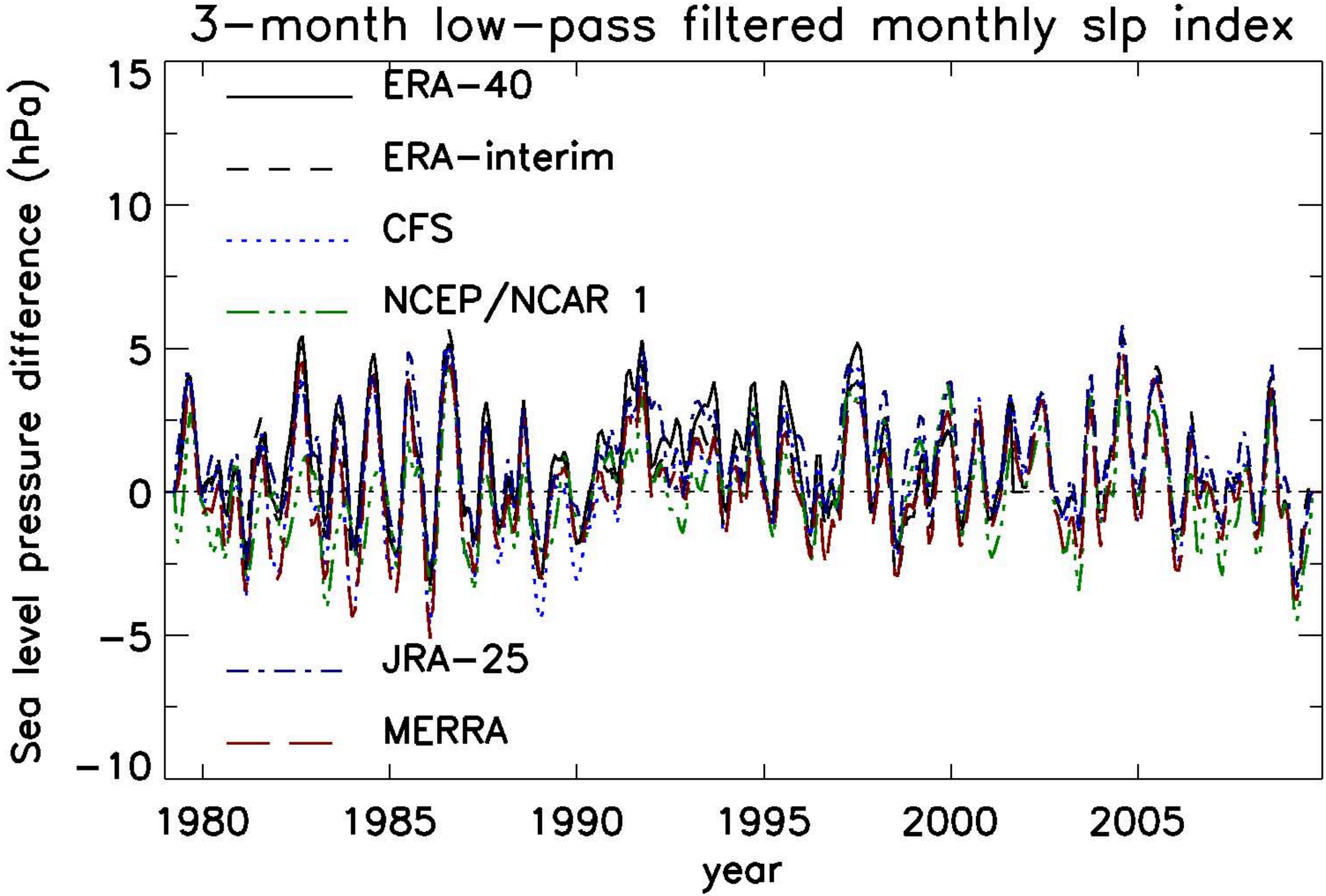
3-month low-pass filtered monthly slp index
Sea level pressure difference (hPa)
15
10
5
0
−5
−10
ERA-40
ERA-interim
CFS
NCEP/NCAR 1
JRA-25
MERRA
1980
1985
1990
1995
2000
2005
year

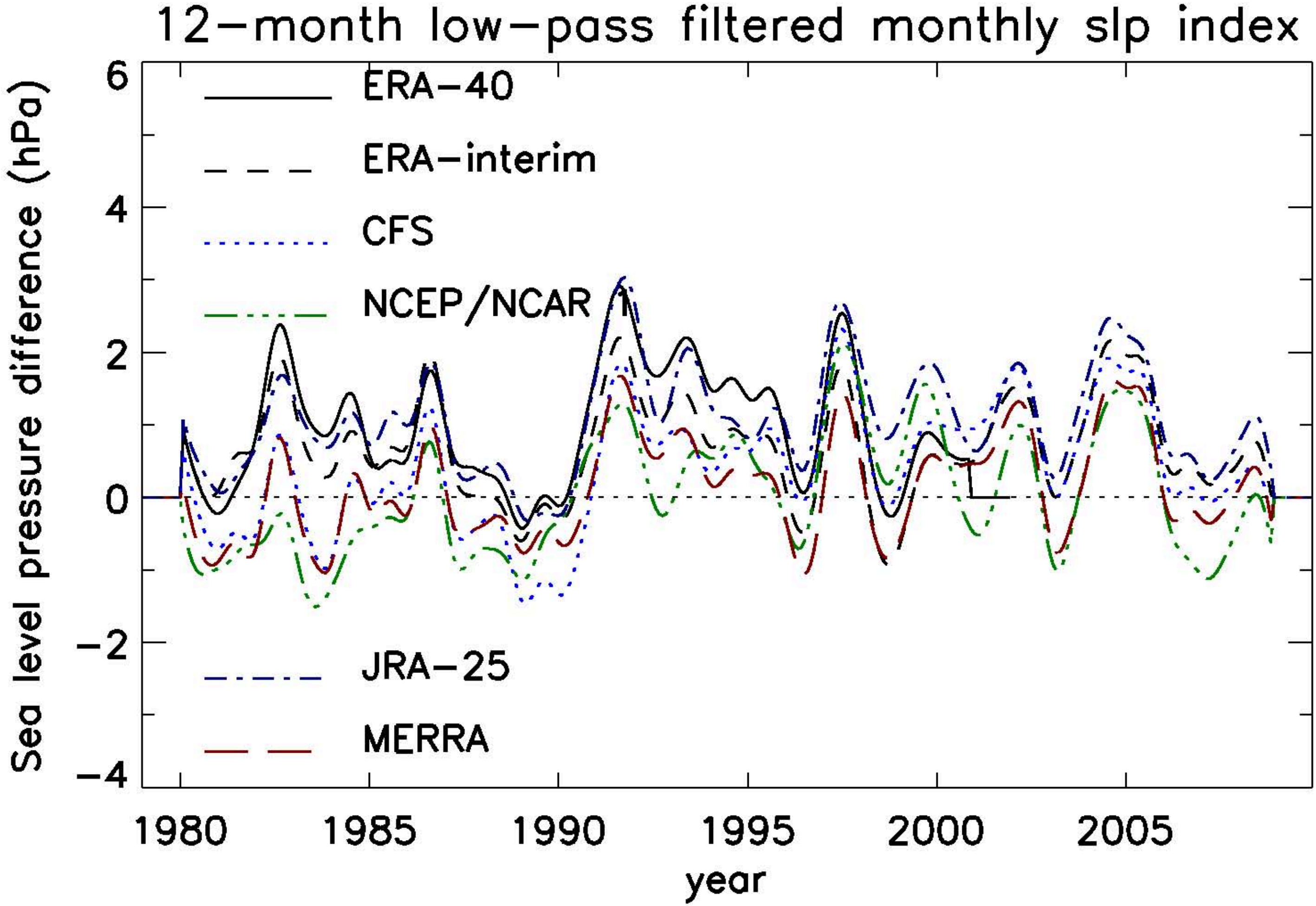
12-month low-pass filtered monthly slp index
ERA-40
ERA-interim
CFS
NCEP/NCAR 1
JRA-25
MERRA
Sea level pressure difference (hPa)
year
6
4
2
0
-2
-4
1980
1985
1990
1995
2000
2005

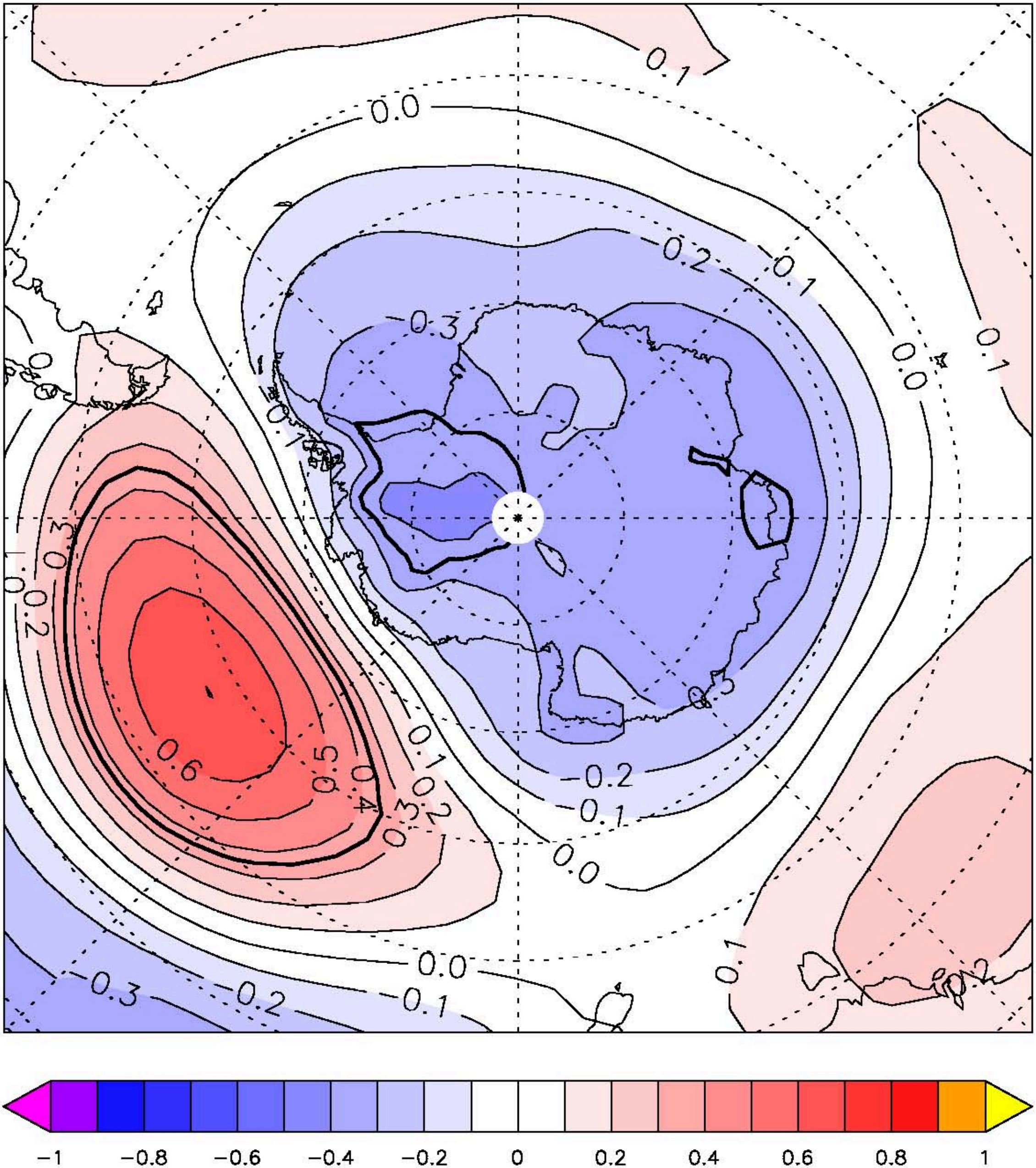

−1
−0.8
−0.6
−0.4
−0.2
0
0.2
0.4
0.6
0.8
1

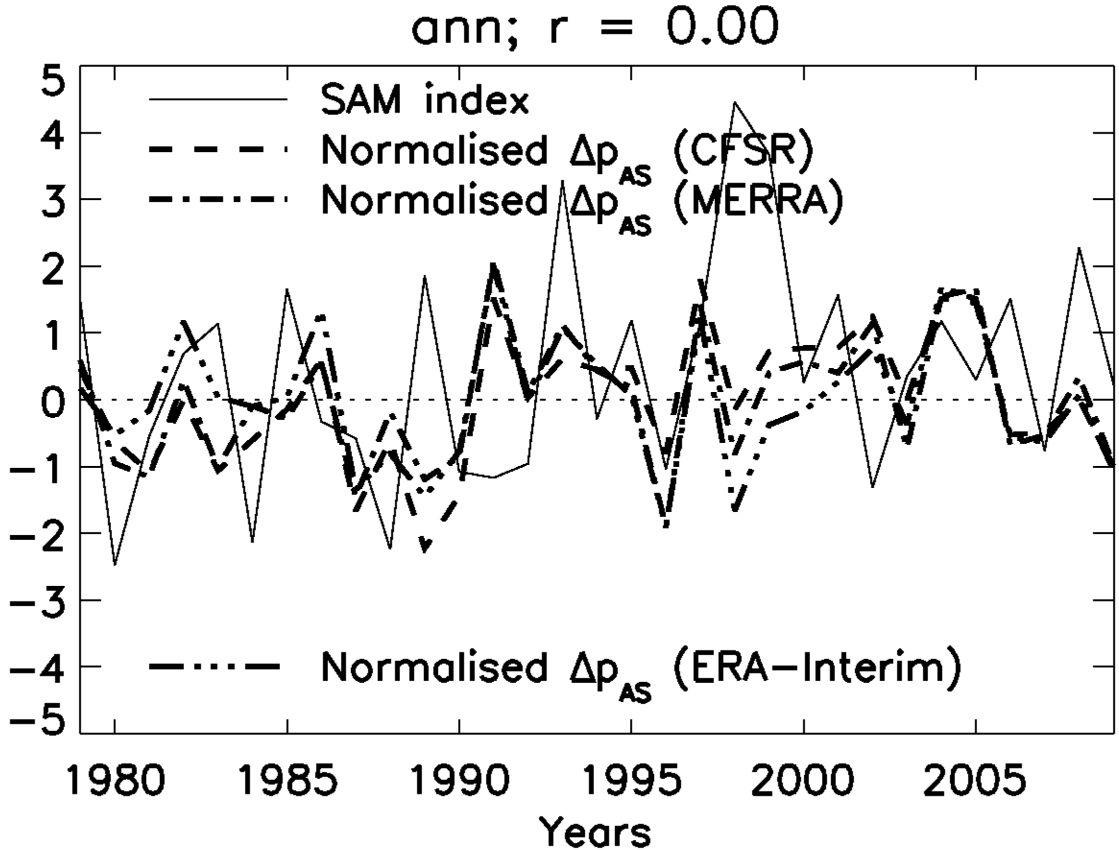

ann; r = 0.00
SAM index
Normalised Δp_AS (CFSR)
Normalised Δp_AS (MERRA)
Normalised Δp_AS (ERA−Interim)
5
4
3
2
1
0
−1
−2
−3
−4
−5
1980
1985
1990
1995
2000
2005
Years

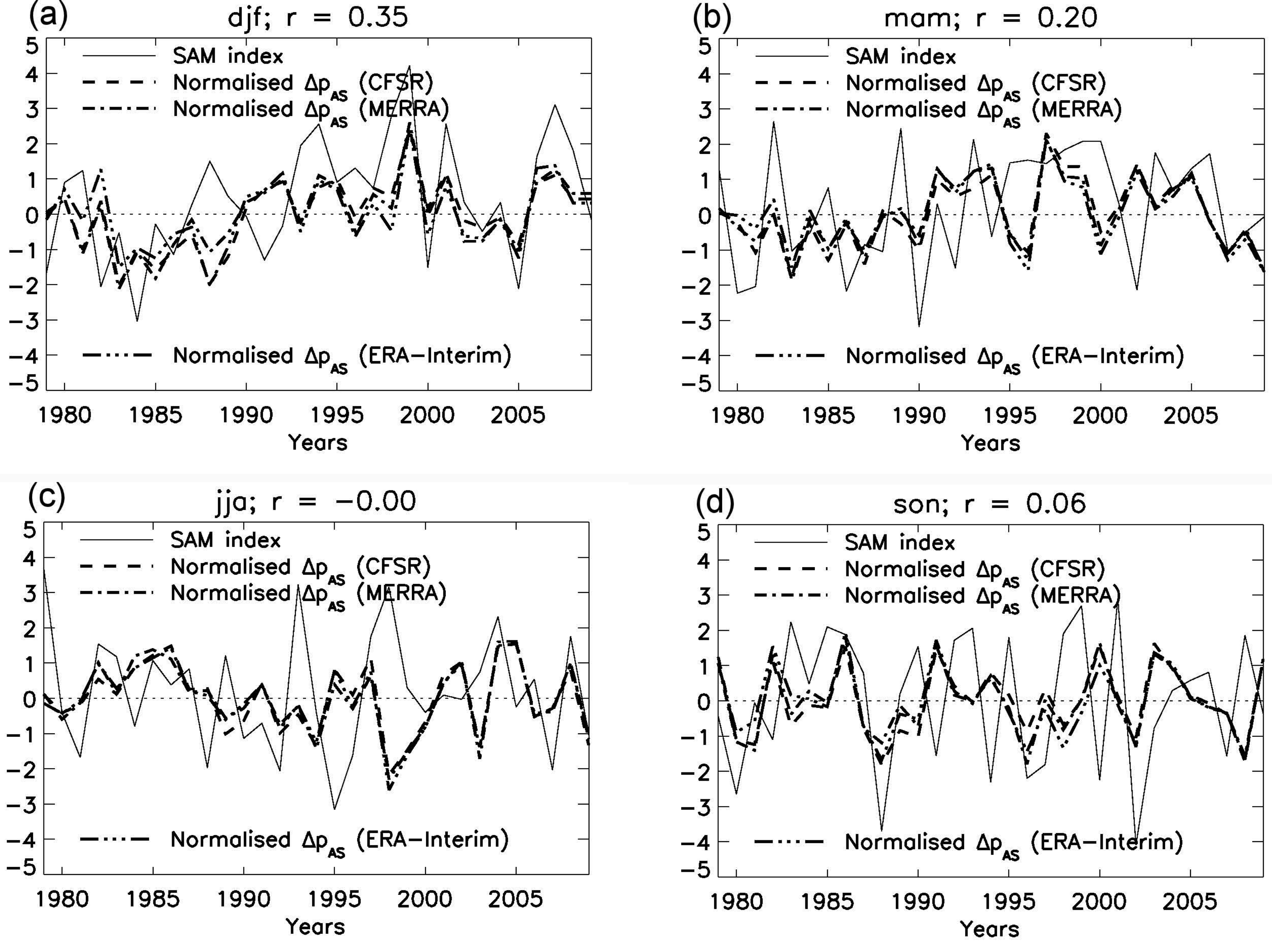

(a)
djf; r = 0.35
SAM index
Normalised Δp_AS (CFSR)
Normalised Δp_AS (MERRA)
Normalised Δp_AS (ERA−Interim)
Years
(b)
mam; r = 0.20
SAM index
Normalised Δp_AS (CFSR)
Normalised Δp_AS (MERRA)
Normalised Δp_AS (ERA−Interim)
Years
(c)
jja; r = −0.00
SAM index
Normalised Δp_AS (CFSR)
Normalised Δp_AS (MERRA)
Normalised Δp_AS (ERA−Interim)
Years
(d)
son; r = 0.06
SAM index
Normalised Δp_AS (CFSR)
Normalised Δp_AS (MERRA)
Normalised Δp_AS (ERA−Interim)
Years